RTP801 Gene Expression Is Differentially Upregulated in Retinopathy and Is Silenced by PF-04523655, a 19-Mer siRNA Directed Against RTP801

Kay D. Rittenhouse,[1] Theodore R. Johnson,[2] Paolo Vicini,[2] Brad Hirakawa,[3] Dalia Kalabat,[3] Amy H. Yang,[3] Wenhu Huang,[3] and Anthony S. Basile[*,4]

[1]Ophthalmology External Research Unit, External R&D Innovations, Pfizer, Inc., San Diego, California
[2]Pharmacokinetics, Dynamics and Metabolism, Pfizer, Inc., San Diego, California
[3]Drug Safety R&D, Pfizer, Inc., San Diego, California
[4]Pfizer, Inc., San Diego, California

Correspondence: Kay D. Rittenhouse, External R&D Innovations, Pfizer, Inc., 10777 Science Center Drive CB4, San Diego, CA 92120; krollins328@gmail.com.

Current affiliation: *Allergan LLC, Irvine, California.

Submitted: October 22, 2013
Accepted: January 10, 2014

Citation: Rittenhouse KD, Johnson TR, Vicini P, et al. RTP801 gene expression is differentially upregulated in retinopathy and is silenced by PF-04523655, a 19-mer SiRNA directed against RTP80. *Invest Ophthalmol Vis Sci*. 2014;55:1232–1240. DOI: 10.1167/iovs.13-13449

Purpose. The intraocular pharmacodynamics of PF-04523655, a small-interfering RNA (siRNA) directed against RTP801, was characterized using rat models of retinopathy.

Methods. Rat models of streptozotocin-induced diabetes and wet AMD were used to determine the onset, extent, and duration of siRNA inhibition of retinal RTP801 expression by PF-04523655, and this inhibition was characterized by pharmacokinetic/pharmacodynamic (PK/PD) modeling. A rat model of wet AMD was also used to examine PF-04523655 dose-dependent effects on the incidence of clinical grade 3 or 4 choroidal neovascularization lesions. Whole homogenate versus laser-capture microdissected (LCM) retinal samples were analyzed by quantitative PCR for RTP801 expression.

Results. RTP801 expression in RPE/choroid (RPE/C) increased in diabetic rats by up to 70% above nondiabetic rat levels. Inhibition of retinal RTP801 expression by PF-04523655 began 1 day after intravitreous injection and was observed through day 7 in the neurosensory retina and through day 14 or longer in RPE/C. PF-04523655 inhibition of RTP801 expression was maintained well after clearance of PF-04523655 from the eye and was best characterized by an effect compartment PK/PD model. Moreover, PF-04523655 administration decreased the incidence of clinical grade 3 or 4 lesions by approximately 60% ($P = 0.053$), and dose-dependently inhibited retinal RTP801 expression ($P < 0.01$). RTP801 expression was enriched in the outer nuclear layer in LCM samples.

Conclusions. In rodent retinopathy models, administration of the siRNA, PF-04523655, reduced RTP801 expression in the retina, consistent with the RNA-induced silencing complex (RISC) mechanism of action. The pharmacodynamic profile from the animal models could be useful to elucidate dose and exposure dependency of RTP801 expression inhibition by siRNA.

Keywords: gene expression, PK/PD, hypoxia, retinal pigment epithelium, retinal ischemia

A therapeutic approach using small-interfering RNA (siRNA) is being evaluated in a number of important diseases, including retinopathies, such as diabetic macular edema (DME) and wet AMD.[1–4] Understanding the complexities of the pharmacokinetics and pharmacodynamics of gene silencing by therapeutic siRNAs is critical for optimizing treatment paradigms for therapeutic success.

RTP801 is an inhibitor of the mammalian target of rampamycin complex 1 (mTORC1) and downstream transcription factor HIF-1.[5–7] RTP801 is a hypoxia-inducible stress response gene,[8,9] and its gene product is expressed in vivo at low, basal levels in a variety of tissues.[8] The sequence of the RTP801 gene is highly conserved, with a high sequence homology between humans and rabbits (94%),[10] humans and rats and mice, (91%; accession nos. Q9X09 [humans]; Q9D3F7 [mouse]; Q8VHZ9 [rat]), and humans and monkeys (99%); accession no. F7DLT7) as determined by Basic Local Alignment Search Tool (BLAST) analysis (www.uniprot.org). RTP801, also known as REDD1, is a stress-response gene[8,9] that is induced in diseases such as Parkinson's disease,[11,12] and under conditions such as smoke inhalation.[7,13] Exploratory studies of other ischemic disease mechanisms and disease models, such as the middle cerebral artery occlusion model of stroke[8] and acute alcohol intoxication,[14] have confirmed RTP801-mediated activity. Ischemia and inflammation are key pathogenic mechanisms contributing to diabetic retinopathy and AMD, respectively.[15–17] As a result, it was postulated that inhibition of RTP801 expression may confer protection against hypoxic or stress-related damage to retinal cells in vitro. Garcia-Manso et al. (Garcia-Manso, et al. *IOVS* 2011;52:ARVO E-Abstract 1424) used an in vitro model of chemically induced hypoxia, confirming that $CoCl_2$ insult induced RTP801 expression that was inhibited by PF-04523655. The relevance of this target in retinal disease in vivo was demonstrated in a RTP801 knock-out (KO) mouse model of retinopathy of prematurity,[18] where an approximately 80% reduction in capillary free areas in the retina was observed in KO mice versus wild-type mice. Similarly, retinal neovascularization decreased by approximately 60% in KO mice versus wild-type mice. Thus, inhibition of RTP801 expression

may play a role in ameliorating retinopathies, such as diabetic retinopathy and AMD.

PF-04523655 is a 19-ribonucleotide double-stranded siRNA designed for sequence-specific inhibition of RTP801 gene transcription, and has been *O*-methyl modified to enhance its enzymatic stability. PF-04523655 has been studied in Phase 2 clinical trials for efficacy in treating wet AMD[2,19] and DME.[3]

This article reports the results of a series of nonclinical studies conducted to confirm the relevance of RTP801 expression in retinopathy and to describe the in vivo exposure-response relationships for PF-04523655 inhibition of retinal RTP801 expression in models of retinopathy. In the first study, a diabetic rat model was used to examine whether RTP801 expression was upregulated in the ischemic retina. Second, a study was conducted to examine whether an siRNA directed against RTP801, PF-04523655, would inhibit this expression in diabetic rats, while also characterizing the onset, extent, and duration of inhibition after a single intraocular low dose. Next, pharmacokinetic/pharmacodynamic (PK/PD) modeling of exposure and retinal expression data, respectively, was conducted to elucidate the parameter estimates useful for quantifying the exposure/response relationship for RTP801 inhibition in the retina by PF-04523655. Then, a laser-induced choroidal neovascularization (CNV) model was used to develop a dose-response curve for both retinopathy as assessed by clinical grade 3 to 4 lesion scores and for the attenuation of retinal RTP801 expression. Finally, quantitative PCR (qPCR) analysis of retina samples obtained by laser-capture microdissected (LCM) capture of inner nuclear layer (INL), outer plexiform layer (OPL), outer nuclear layer (ONL), and RPE in control and diabetic rats was conducted to further understand the regional distribution of RTP801 expression within subretinal layers in comparison with intact neurosensory retina or RPE/choroid (RPE/C) homogenates to provide further clarity on the study results.

Methods

The term "retina" is used to refer to neurosensory retina (all neuronal layers) plus RPE/C, unless specifically noted. Where specifically noted, the use of RPE isolated from choroid (i.e., in LCM experiment) is also be described.

Retinopathy Models

Streptozotocin-Induced Rat Diabetic Retinopathy Model. Streptozotocin (STZ; 50 mg/kg intravenous [IV]) was administered to Long Evans rats. Rats were considered diabetic after achieving blood glucose levels of 250 mg/dL or higher after a minimum of 3 days or up to a maximum of 14 days after STZ administration. Control rats were administered IV saline injections and received identical incubation periods as the experimental groups.

Laser-Induced CNV Model of Wet AMD in Rats. Anesthetized Long Evans rats received a 4- to 6-spot laser pattern between the major retinal vessels around the optic disc of each eye using an 810-nm diode laser at an initial power setting of 300 mW and a duration of 0.05 to 0.1 seconds, to generate a spot size of 80 to 100 μm. Rupture of Bruch's membrane was confirmed by observation of a vaporization bubble in the retina during the laser procedure.

Animals used in these studies were managed in facilities according to ARVO guidelines.

RTP801 Expression in STZ-Induced Diabetes

Vehicle-treated control (IV saline) versus STZ-treated rats (n = 12/time point/group; STZ dose: 50 mg/kg IV) were euthanized on days 8 and 29 (vehicle-treated control groups only), and day 8, day 15, day 22, and day 29 (STZ-treated groups). Following euthanasia, retina and RPE/C tissues were collected, and RTP801 expression was measured using qPCR analysis. Day 8 and 29 RTP801 expression samples for vehicle-treated groups were pooled for comparison with the STZ-treated groups.

Time Course of PF-04523655 Inhibition of RTP801 Retinal Expression in a Rat Model of STZ-Induced Diabetes

STZ-treated rats (n = 12 per group) received PF-04523655 (10 μg/eye intravitreal injection [IVT]) after onset of diabetes (day 14). Following euthanasia on days 15, 22, 29, and 43, retina and RPE/C were collected and analyzed using qPCR.

PK/PD Analysis of the Time Course of PF-04523655 Inhibition of Retinal RTP801 Expression

Rats were administered a single 50-μg/eye IVT dose of PF-04523655 (sense strand: 5′-GUGCCAACCUGAUGCAGCU-3′; antisense strand: 3′-CACGGUUGGACUACGUCGA-5′). At specific time intervals after dosing (1, 8, 24, 48, 96, 168, and 240 hours post dose), rats (n = 3 per time point) were euthanized and vitreous, retina, RPE/C, and plasma samples were collected.

Ocular tissue and plasma samples were assayed using a dual-hybridization method. Briefly, samples containing PF-04523655 were heat denatured (90°C) to liberate the antisense strand of PF-04523655 from its complementary sense strand in the duplex. The 3′-end of the antisense strand of PF-04523655 was hybridized to a 10-base complementary oligonucleotide (i.e., capture probe; 5′-GUGCCAACCU-3′), and the 5′-end was hybridized to another 9-base complementary oligonucleotide (i.e., detection probe; 5′-GAUGCAGCU-3′). The capture probe included an amine group at the 5′-terminus, which allowed it to be covalently tethered to the surface of a DNA-BIND 96-well plate (Corning, Inc., Acton, MA). The detection probe contained two biotin groups at the 3′-end. The capture and detection probes were composed solely of lock nucleic acid nucleotides to increase the binding affinity to the target PF-04523655. Initially, the liberated antisense strand of PF-04523655 was hybridized with the detection probe. The complex of PF-04523655 antisense strand/detection probe was transferred to the capture probe-coated DNA-BIND 96-well plate, and the unbound portion of PF-04523655 (3′-terminus) left to anneal with the capture probe to form a "sandwich complex." Measurement of surface-bound PF-04523655 was performed via detection of the free biotin groups on the detection probe, using streptavidin conjugated to horseradish peroxidase, which catalyzed the 3,3′,5,5′-tetramethylbenzidine substrate. Colorimetric intensity was measured using a Spectramax 340PC and PLUS384 plate readers (Molecular Devices, Sunnyvale, CA), and the signal was proportional to the amount of PF-04523655 present in the samples. The lower limits of quantification (LLOQ) were 5 ng/mL for vitreous, 10 ng/g for retina and RPE/C, and 0.1 ng/mL for plasma.

Noncompartmental PK parameters were determined from composite concentration-time data using WinNonlin (Pharsight Corporation, St. Louis, MO). PK/PD modeling was conducted by using the PK data (scaled to 10 μg from 50 μg, assuming linear kinetics) and PD data from the RTP801 expression levels following administration of PF-04523655 (10 μg IVT) to STZ-induced diabetic rats. A PK compartmental model was developed to estimate exposures in retina and RPE/C based on observed data. Tissue volumes of distribution were assumed based on literature-reported values, and the model rate

Investigative Ophthalmology & Visual Science

constants were simultaneously fit to pooled available sample measurements (plasma, vitreous, retina, and RPE/C). PF-04523655 concentration predictions were used in the pharmacodynamic modeling. Transient baseline elevation of RTP801 expression in both retina and RPE/C after STZ injection was modeled from control experiments as an exponentially decreasing slope (B[t]).

Modeled PK exposures were then paired with a link-E_{max} model to estimate PD parameters of PF-04523655 from pooled RTP801 expression data. The PK/PD model included a pharmacodynamic delay for either retina or RPE/C concentration, described as concentration in the effect compartment (Ce(t)), where C(t) is either retina- or RPE/C-predicted exposure. The pharmacodynamic delay rate parameter is denoted as k_{eo}. The pharmacodynamic model for gene expression[20] is an E_{max} model, in which the pharmacodynamic modulation is linked to C(t) through Ce(t). It was assumed that the effect on gene expression is mediated through an effect site concentration, Ce(t), which is remote from the measured exposure (either retina or RPE/C).

Evaluation of PF-04523655 Dose-Related Inhibition of RTP801 Retinal Expression and Relationship to CNV Lesions in a Rat Model of Wet AMD

Shortly after laser treatment on day 1 and secondarily on day 8, rats were administered vehicle (IVT saline) or PF-04523655 (1, 2.5, or 50 μg/eye) by IVT in 1-μL injections. On day 15, the individual laser spots on the still images were evaluated for leakage using a semiquantitative scale of 0 to 4 by two independent readers who were masked to treatment, and who subsequently determined a consensus score according to the following ratings:

- 0 = no leakage (only laser scar or very diffuse small hyperfluorescent area visible);
- 1 = minimal leakage (small areas of diffuse or solid hyperfluorescence generally remaining within the laser-induced defect region);
- 2 = slight leakage (semisolid hyperfluorescence generally remaining within the boundary of the laser-induced defect region);
- 3 = moderate leakage (semisolid to solid hyperfluorescence generally remaining within the boundary of the laser-induced defect region); and
- 4 = Substantial leakage (solid hyperfluorescent region extending beyond the boundary of the laser-induced defect region).

Rats were euthanized and neurosensory retina and RPE/C were collected and assayed for RTP801 gene expression using qPCR.

LCM and qPCR of RTP801 Expression

All prior studies described above, where qPCR analysis was performed, except for the LCM samples, involved the analysis of whole neurosensory retina or whole RPE/C homogenate. For the LCM samples, the following analysis procedure was used: The localization of the RTP801 mRNA expression in retinas of normal ($n = 2$ eyes) and diabetic rats ($n = 2$ eyes; STZ 50 mg/kg IV) was determined in LCM samples taken from the INL, OPL, ONL, RPE, and retina cross-section followed by qPCR. Immediately after euthanasia, eyes were embedded in cryomolds containing OCT compound (Sakura Finetek, Torrance, CA), frozen in an isopentane–dry ice bath, and then stored at –80°C. Tissue sections were cut on a Leica CM1950 cryostat (Buffalo Grove, IL) and collected on RNase-free glass slides (Arcturus PEN membrane; Applied Biosystems, Foster City, CA). For hematoxylin and eosin staining, sections were placed in decreasing concentrations of ethanol (from 100% down to 50%) in stepwise fashion, followed by hematoxylin, 50% ethanol, eosin, de-stained and then dehydrated in xylene and ethanol. Immediately after staining, different retinal layers were sampled using LCM (Arcturus Veritas system; Applied Biosystems), and the samples were collected separately from each animal using Macro LCM caps (Arcturus CapSure; Applied Biosystems). The caps were then processed to stabilize the RNA and frozen at –80°C until RNA extraction. For the RNA amplification and gene expression analysis, total RNA was extracted from the LCM samples (Arcturus PicoPure RNA isolation kit; Applied Biosystems) and evaluated (2100 Bioanalyzer, RNA 6000 Pico kit; Agilant Technologies, Santa Clara, CA). Total RNA was amplified to generate cDNA (WT Ovation Pico SL WTA system; NuGen, San Carlos, CA), such that 6 to 8 μg cDNA was generated from 500 pg of RNA. The amplified cDNA was then used in the qPCR analysis using primers and probes specific to the RTP801 gene (catalog no. Rn00590207; Applied Biosystems), which was validated at Pfizer (San Diego, CA) using LCM samples and to the β-actin housekeeping gene that was designed by Pfizer and produced by IDT Technologies (San Diego, CA). The β-actin probe sequence was 5′-/56-FAM/ATC AAG ATC ATT GCT CCT CCT GAG CGC/36-TAMSp/-3′. The forward and reverse primers were TGGCTCCTAGCACCAT and ACCAATCCACACAGAG TACT, respectively. qPCR analysis (qScript qRT-PCR; Quanta Biosciences, Inc., Gaithersburg, MD) was performed using total RNA on a LightCycler 480 (Roche, Indianapolis, IN).

qPCR Analysis of RTP801 Gene Expression in Whole Retina Homogenate Samples

qPCR analysis was performed on total RNA extracted from selected ocular tissues (neurosensory retina, RPE/C) for all studies except the LCM analysis work (described in the previous section). Briefly, frozen tissues were thawed, removed from the preservative (RNAlater), and placed in Qiazol reagent (Qiagen, Valencia, CA) for subsequent dissociation in a bead-mill homogenizer. Samples were mixed thoroughly after the addition of chloroform (Sigma, St. Louis, MO) and then centrifuged under refrigeration. The clear supernatant was added to a M48 Biorobot (Qiagen) for purification of total RNA. The probe and primers for analysis of the RTP801 gene were designed using Roche Universal Probe Library (UPL) software (Roche). UPL probe number 116 (catalog no. 0463507001) was used in conjunction with forward (CCAGAGAA GAGGGCCTTGA) and reverse primers (CCATCCAGGTATGAG GAGTCTT; IDT Technologies). Roche probe and primers were selected because they were validated previously at Pfizer using whole retina homogenate samples. The probe and primer for analysis of the housekeeping gene β-actin were designed by Pfizer and produced by IDT Technologies. The probe sequence was 5′-/56-FAM/ATC AAG ATC ATT GCT CCT CCT GAG CGC/36-TAMSp/-3′. The forward and reverse primers were TGGCTCCTAGCACCAT and ACCAATCCACACAGAGTACT, respectively. qPCR analysis (qScript qRT-PCR; Quanta Biosciences, Inc.) was performed using total RNA on a LightCycler 480 (Roche). Beta actin was selected for normalizing gene expression because of precedent from the scientific literature,[21] and verification of stable gene expression across all siRNA dose groups and target tissues within our series of studies. Other typical markers used for normalization were evaluated, such as glyceraldehyde 3-phosphate dehydrogenase, but were not chosen due to lack of stable gene expression. Raw data were exported from the LightCycler 480 to Microsoft

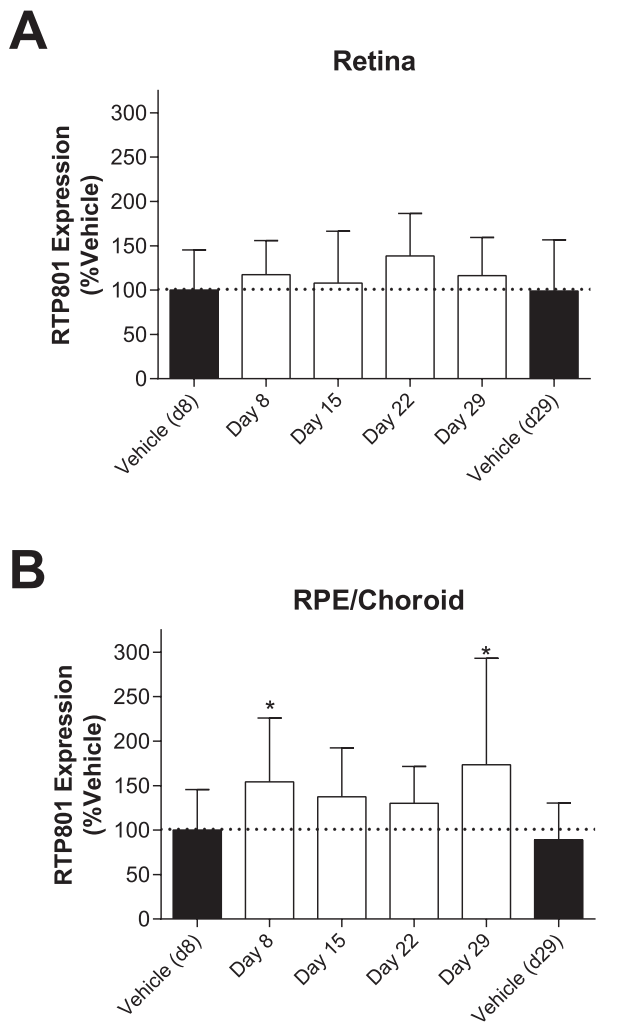

Figure 1. Time course of RTP801 expression retina (**A**) and RPE/C (**B**) in STZ treated rats. *$P < 0.05$. *Dashed line* represents %RTP801 expression in control (vehicle-treated) animals. Time scale is expressed as day postcommencement of STZ dosing.

Excel (Microsoft, Redmond, WA) for sorting into appropriate experimental groups.

The following contract research organizations were used for the conduct of aspects of this work: Charles River Laboratories (Montreal, Quebec, Canada), rodent laser CNV and rodent STZ diabetic rat in vivo studies and ocular tissue dissections, and bioanalysis of ocular tissues for PF-04523655 levels; and Covance Laboratories (Madison, WI), rodent ocular PK in vivo studies and ocular tissue dissections. Intact retinal tissues (retina and RPE/C) were harvested from the in vivo experiments conducted at Charles River Laboratories. The tissues were homogenized and qPCR analysis of homogenates was performed at Pfizer (La Jolla, CA). The in vivo studies in STZ-treated versus normal rats, ocular dissections, LCM retinal subregion sampling, and subsequent qPCR analysis was conducted by Pfizer.

Statistical Analysis

qPCR data were imported into GraphPad Prism (La Jolla, CA) for statistical analysis. A one-way ANOVA was performed using Dunnett's multiple comparison test to assess between-group differences in ocular tissue RTP801 expression by qPCR. Differences were considered statistically significant at P less than 0.05. For STZ-treated animals, rats were excluded from analysis if the blood glucose ($\geq$250 mg/dL) criterion for the definition of diabetes was not met. For the laser CNV-treated rats, a two-sided Fisher's exact test for count data was used to characterize group differences in the incidence of grade 3 to 4 lesions as a function of dose. For the PK and PK/PD analyses, WinNonlin software and SAAM II software (the Epsilon Group, Charlottesville, VA) were used to model exposure and response characteristics.

Results

RTP801 expression did not change significantly within neurosensory retina of diabetic rats relative to vehicle-treated rats over the 28-day sampling period. However, there was a numeric increase (~50%) in the level of RTP801 mRNA expression in the retina on day 22 (Fig. 1A). In contrast, diabetic rats had statistically significant increases in RTP801 expression in RPE/C on days 8 and 29 ($P < 0.05$) of up to 70% over vehicle-treated rats (Fig. 1B).

PF-04523655–mediated attenuation of RTP801 expression as a function of time after the induction of diabetes was examined. PF-04523655 reduced RTP801 expression levels by the first observation period, 1 day after administration, in both the retina and RPE/C, with reduced expression through day 8. Fourteen days later, retina RTP801 expression returned to

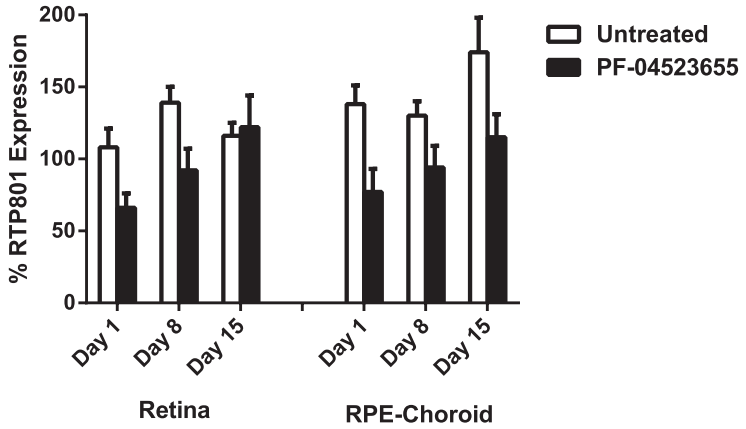

Figure 2. Time-course of RTP801 expression in retina or RPE-choroid from STZ-induced diabetic rats following no treatment (*open bars*) or IVT administration of 10 μg/eye PF-04523655 (*solid bars*). Time scale is expressed as day post PF-04523655 dose. Mean values ± SEM (n = ~24 eyes/group).

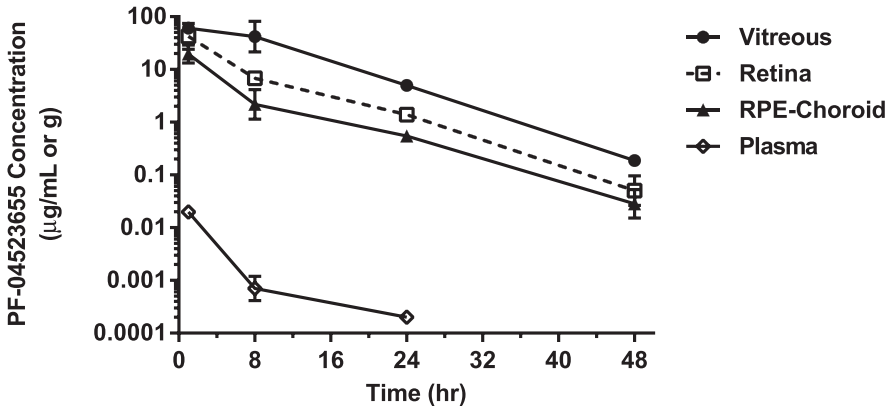

FIGURE 3. Concentration versus time profiles of PF-04523655 in ocular tissues and plasma following a 50 μg/eye IVT dose of PF-04523655. Mean data ± SD ($n = 3$/time point).

pretreated levels, while RPE/C expression remained decreased (Fig. 2).

The pharmacokinetics of PF-04523655 were determined from concentration versus time profiles in vitreous humor, retina, RPE/C, and plasma in normal rats following PF-04523655 (50 μg/eye, IVT). A gradient of PF-04523655 distribution through the eye was observed: maximal concentrations (C_{max}) were highest in vitreous, followed by the retina, and RPE/C (Fig. 3; Table). PF-04523655 was detectable in the plasma at the earliest time point (1 hour) after IVT, but at concentrations more than 1000 times lower than in the eye (Table). Once PF-04523655 enters the plasma, it is rapidly diluted/metabolized. The volume of distribution in vitreous was approximately 10-fold greater than the physiological volume (50 μL) in rats, indicating the distribution of PF-04523655 beyond the vitreous compartment. The elimination half-life ($t_{½}$) values of PF-04523655 were relatively consistent across all ocular tissues and plasma at 4 to 6 hours, shorter than those observed in rabbits (~30–40 hours; Johnson TR. *IOVS* 2010;51:ARVO E-Abstract 2442). In contrast to the relatively short ocular PK $t_{½}$ in the rat, maximal RTP801 transcriptional attenuation was maintained for 7 or more days in the retina and RPE/C after PF-04523655 administration (Fig. 4), while ocular tissue concentrations of PF-04523655 were below the LLOQ. The relationship between PF-04523655 levels in the retina or RPE/C and inhibition of RTP801 expression was characterized with a link-E_{max} model (Fig. 5). Based on these analyses, PF-04523655 potently inhibited RTP801 expression, with half maximal effective concentration (EC50) values ranging from 4 to 18 ng/mL. The maximal inhibition of RTP801 expression (E_{max}) was estimated at 46% and 85% in retina and RPE/C, respectively. The substantial observed variability in RTP801 expression data (Fig. 4) was reflected in the sometimes poor (>100%) individual parameter precision. The k_{eo} values,[12] reflecting the distributional delay rate constant between the PK and effect compartments, suggested slower equilibration and longer distributional delay for RPE/C relative to retina. The distributional delay half-life values ($t_{½}$ corresponding to the k_{eo} estimate) in retina and RPE/C were 20 ($k_{eo} = 0.035$ hour^{-1}) and 70 hours ($k_{eo} = 0.010$ hour^{-1}), respectively, 3- to 17-fold longer than the corresponding PK $t_{½}$ values in these tissues.

RTP801 gene expression in the retinas of rats with laser-induced CNV was dose-dependently inhibited up to 50% relative to vehicle controls ($P < 0.01$; Fig. 6A) after IVT PF-04523655 administration. However, this was not observed in RPE/C (Fig. 6B). PF-04523655 reduced grade 3 to 4 CNV lesions by approximately 60% on average ($P = 0.053$), although inhibition was not dose related (Fig. 7).

Because whole tissue homogenate preparations were collected and assayed by qPCR, with probable dilution of expression, LCM was used to assess regional distribution of RTP801 expression within specific layers of the retina (INL, OPL, ONL, and RPE; Fig. 8A) and compared with results from cross-sectional retina samples (Fig. 8B, labeled RET). The differences in RTP801 expression of the corresponding LCM sections obtained from normal and STZ-treated rats ($n = 2$ eyes per group), were minimal. However, the averaged level of expression per region using all rats confirmed ONL expression was approximately 6-fold higher than the next-highest samples of expression, neurosensory retina, confirming the apparent dilution of expression signaling (Fig. 8B).

DISCUSSION

Bridging from studies in a murine RTP801 knock-out model of retinopathy of prematurity, where Brafman et al.[18] showed that the absence of the RTP801 gene conferred protection from retinopathy under ischemic conditions, further mechanistic evaluation of the beneficial effects of the inhibition of RTP801 expression was conducted with the use of the diabetic rat and a rodent model of wet AMD. In this article, we described a series of studies that characterized the role of RTP801 in retinal

TABLE. Noncompartmental Pharmacokinetic Parameters of PF-04523655 in Ocular Tissues and Plasma in Rats After a 50-μg IVT Dose of PF-04523655

Tissue	T_{max}, h	C_{max}, μg/mL	$AUC_{(0\text{-}t)}$, μg·h/mL	$t_{1/2}$, h	CL, mL/h	V_{ss}, mL
Vitreous	—	60.3 ± 7.9	858 ± 276	5.1	0.058	0.45
Retina	1	42.4 ± 18.8	276 ± 92.7	5.6	—	—
RPE-choroid	1	19.7 ± 5.4	115 ± 26	6.3	—	—
Plasma	1	0.020 ± 0.002	0.089 ± 0.008	3.7	—	—

—, not estimated.

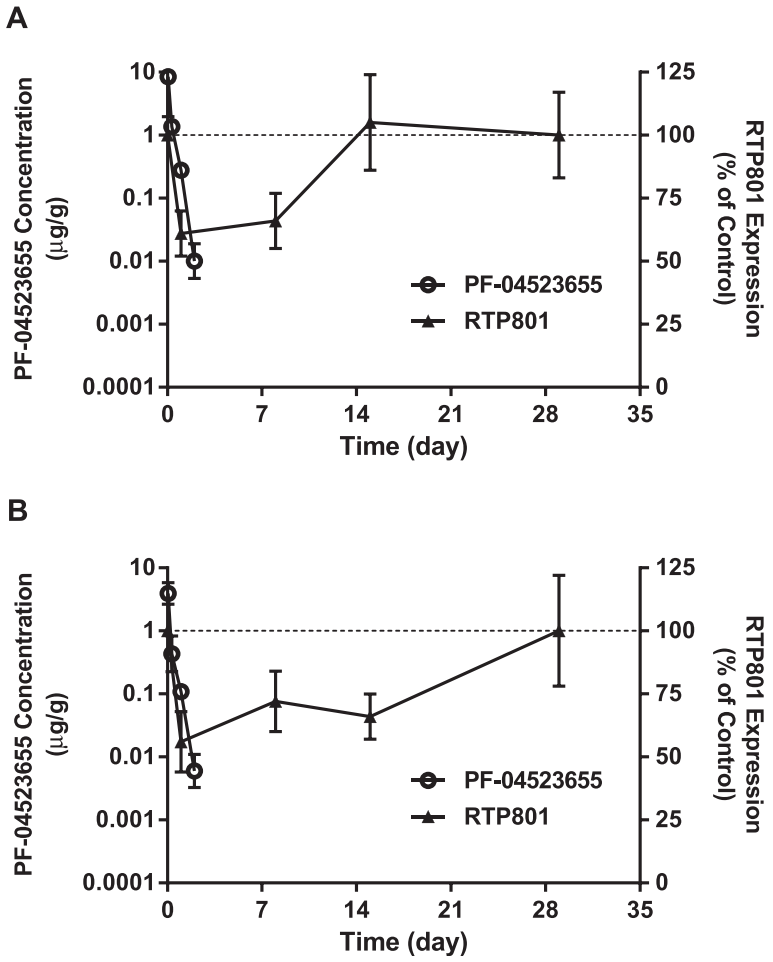

FIGURE 4. PK/PD relationship of PF-04523655 concentration and RTP801 expression in retina (**A**) or RPE/C (**B**) from STZ-induced diabetic rats administered 10 μg/eye PF-04523655. Mean data ± SD (PF-04523655 concentration) or SE (RTP801 expression). RTP801 expression levels were normalized to time-matched values in non–PF-04523655–treated diabetic rats (control group).

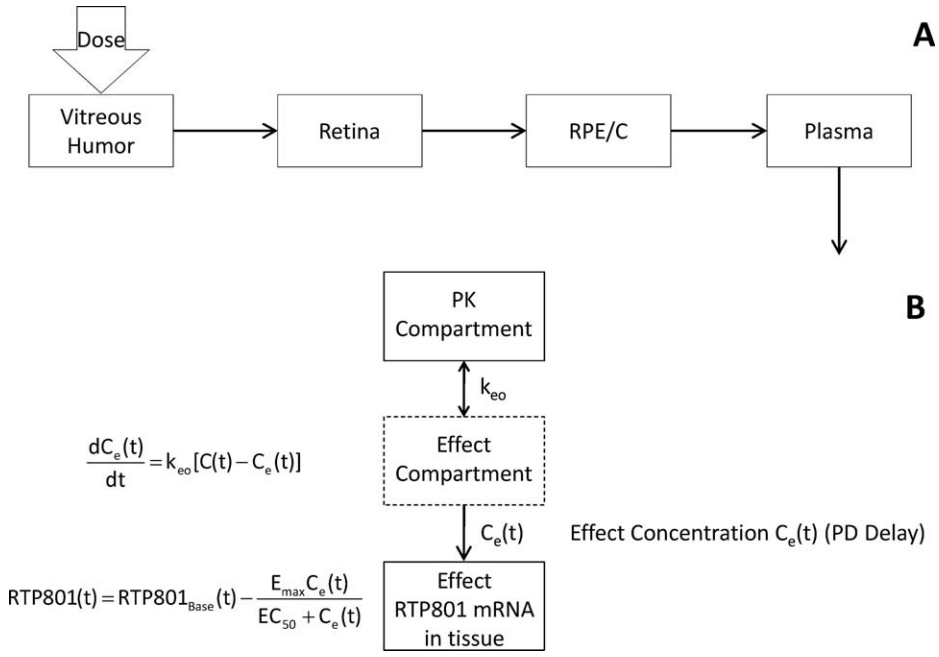

FIGURE 5. Schematic models of (**A**) PF-04523655 clearance from ocular compartments, and (**B**) PK-PD model used to characterize PF-04523655 effects on RTP801 gene expression. PK compartment in (**B**) is either retina or RPE/C concentration, and RTP801(t) indicates gene expression in either retina or RPE/C.

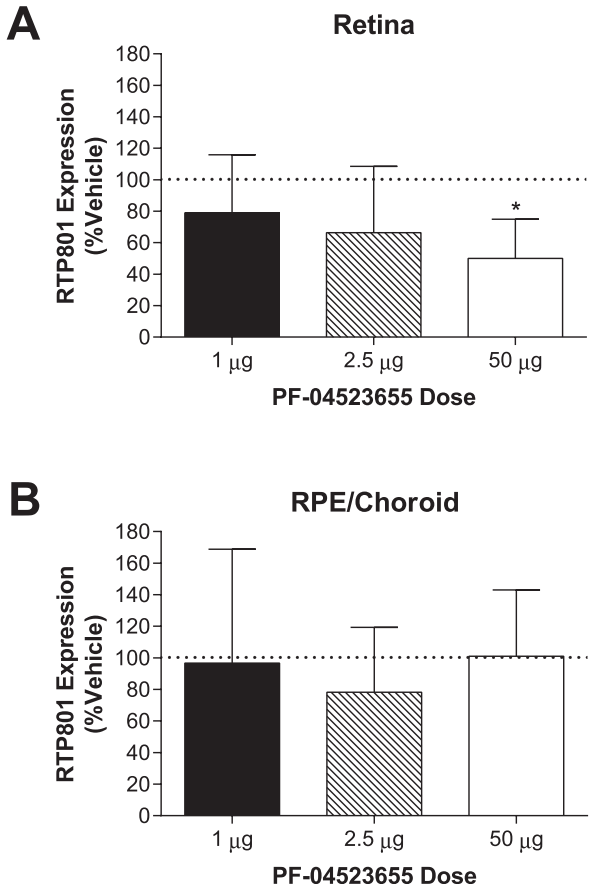

FIGURE 6. Dose-related RTP801 retina (**A**) and RPE/C (**B**) expression normalized to vehicle control (day 15) in laser-induced CNV rats following IVT administration of PF-04523655 (1, 2.5, or 50 µg/eye) in rats. $^{*}P < 0.01$.

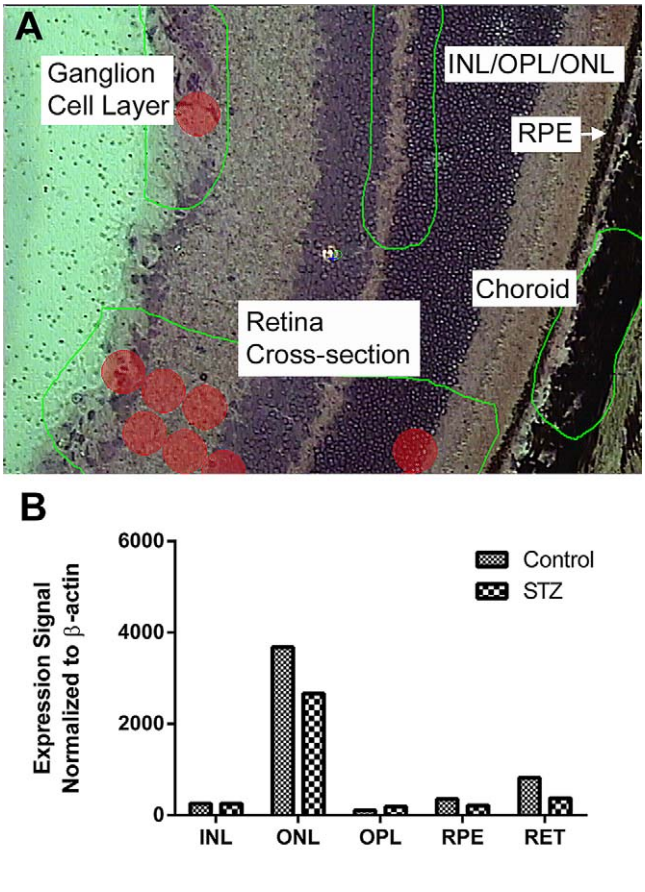

FIGURE 8. LCM photomicrograph of the retina with labeled sample sections. Magnification ×20 (**A**). Diabetic rat versus normal rat RTP801 expression profiles in the retina after LCM (**B**). *Bar graph* depicts the average of two eyes per each group.

diseases, the effect of the attenuation of RTP801 expression in these retinopathies with an siRNA approach, and elucidated the PK/PD relationship of a specific siRNA directed against RTP801, PF-04523655.

RTP801 expression in the diabetic rat was characterized and in vivo dose-response profiles of PF-04523655 transcriptional silencing activity were quantified using a PK/PD model. RPE/C RTP801 expression was upregulated as early as 8 days in STZ-induced diabetic rats, whereas in the retina, expression was numerically increased by day 22. These observations lend credence to investigating the potential therapeutic benefit of inhibition of RTP801 expression in the retina.

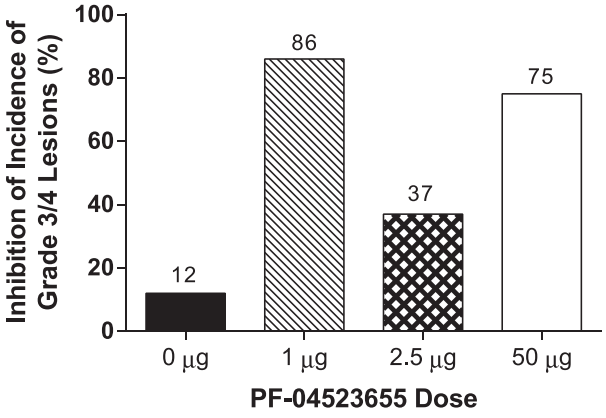

FIGURE 7. Inhibition in incidence of grade 3 to 4 CNV lesions (day 15) in rats following IVT administration of 1, 2.5, or 50 µg/eye PF-04523655 ($n = 8$ eyes/group).

PF-04523655 reduced retina and RPE/C RTP801 expression 1 day after administration (10 µg/eye; IVT) with inhibition that persisted through day 7 in the retina and through day 14, the last observation period, in RPE/C. PK/PD modeling indicated that the pharmacodynamic $t_{½}$ of transcriptional attenuation of retinal RTP801 is 3- to 17-fold longer than the pharmacokinetic $t_{½}$ in the corresponding ocular tissues. This observation is consistent with the sequestration of PF-04523655 into the RISC (RNA-induced silencing complex[22]) that inhibits RTP801 mRNA for a far longer period of time than required by the presence of free PF-04523655 in the vitreous. Other estimates from the PK-PD model were not as reliable (coefficient of variation [CV] > 100%), likely due to the substantial biological variability in RTP801 levels or the potential dilution of expression with homogenate sampling of retinal tissues. Other approaches, such as nonlinear mixed-effects models, may allow a better separation of intersubject variability and measurement uncertainty.

Bartlett and Davis[23] provided a robust evaluation of the kinetics of siRNA gene silencing activity in vitro, establishing the boundary conditions for understanding onset and duration of response based on cell type for the RISC mechanism of action.[22] Their conclusions were in stark contrast to other hypotheses offered to explain the major contribution to siRNA

half-life, namely oligonucleotide structural vulnerability to enzymatic degradation (e.g., endo- or exonucleases). Rather, Bartlett and Davis' study[23] concluded that cell type, that is, whether cell division was possible, was the major factor influencing duration of transcriptional attenuation with siRNAs by the RISC complex. Because neurons comprise a substantial part of the retina, this tissue would constitute an optimal target for an siRNA-targeted therapeutic approach. Indeed, transcriptional silencing appears to persist days to weeks beyond the exposure of PF-04523655 in retinal tissues, likely due to the lack of dilution of RISC machinery, as these cells do not divide. Depending on the activated RISC intracellular degradation rate, persistence of siRNA transcriptional silencing in nondividing cells may be the major factor contributing to the prolonged pharmacodynamic effects of PF-04523655 in comparison with the ocular pharmacokinetics of PF-04523655 in the rat.

PF-04523655 inhibited RTP801 expression in a dose-related manner in the retina, and this activity was linked to a drug-related inhibition in incidence of clinically relevant grade 3 to 4 CNV lesions in the rat (~60%; $P = 0.053$). However, unexpectedly, PF-04523655 did not reduce RTP801 expression in RPE/C, a key tissue implicated in the pathogenesis of AMD. The laser-induced damage in the rodent model may selectively increase RTP801 expression in either the RPE or choroid or neurosensory retina. Thus, homogenization of RPE/C together could result in expression signals from the choroid masking those from the RPE, as the mass of RPE relative to the other tissues is quite small. However, the interpretation of the results from the present set of studies, where differences in the RTP801 expression profile in whole retina or RPE/C homogenate samples versus LCM samples of retinal subregions or RPE were noted, may also be influenced by the observation that homogenates of RPE/C were analyzed while LCM captured RPE samples without choroid.

With LCM analysis, higher endogenous ONL expression of RTP801 was observed, greater than all other regions sampled. Likely due to small sample size, differential RTP801 expression in retinas of diabetic versus normal rats ($n = 2$ eyes/group) did not reach statistical significance, in contrast to results obtained with homogenates of whole retina ($n = 12$/group, or 24 eyes/group). However, the higher endogenous ONL expression of RTP801 suggests that photoreceptors may play a role in the pathology of CNV mediated by RTP801. For example, Léveillard et al.[24] described the so-called rod-derived cone viability factor that promotes cone photoreceptor vitality; deficits in this factor may therefore contribute to retinal disease. Although RPE function is critical for photoreceptor survival, the crucial component contributing to the sight-threatening nature of wet AMD is loss of cone photoreceptors as the source of central vision. Alterations in RTP801 expression in the neurosensory retina also may reflect an indirect pathologic change in response to lesions in other ocular tissues, such as the RPE or choroid, which were anticipated to be the origin of the pathologies.

The nature of the therapeutic responses of different tissues to PF-04523655 suggests that RTP801 expression influences multiple pathways across tissue types and retinopathies. Full suppression of RTP801 expression may be beneficial to retinal cell types and, to some extent, cells in the RPE. However, additional networks may be present in the RPE requiring some level of RTP801 expression to recover from the deleterious effects of the lesions in question. Thus, the lack of a classic dose-response relationship for the reduction of the incidence of grade 3 to 4 CNV lesions by PF-04523655 may reflect the following: variability in model responsiveness to treatment; the inherent variability in execution of laser CNV studies; the semiquantitative nature of the end points used (clinical grade 3 or 4 lesions); or the poorly understood relationship between the role of the RTP801 gene in multiple networks generating or ameliorating a pathology and the clinical end points manifested by these pathologies. Furthermore, published work reported that RTP801 overexpression may be protective or pathogenic under ischemic or hypoxic stresses, depending on the type of cells and the conditioning of the cells.[8] Complexity in RTP801-mediated pathogenesis was observed in the current studies, possibly reflecting inherent differences in both cell type (i.e., RPE versus photoreceptor versus choroidal endothelium) and degree and/or contribution of ischemia/hypoxia versus inflammation to the pathogenic disease mechanisms (i.e., wet AMD versus diabetic retinopathy). This complexity in responses may also have contributed to the observation of a bell-shaped dose-response curve in the laser CNV model and the different responses to siRNA treatment and time course of inhibition of RTP801 expression in diabetic retinopathy versus wet AMD in the rodent models.

The results reported in this article demonstrated that alterations in RTP801 expression are associated with diabetic and AMD retinopathy in rat models. The pharmacological effects of PF-04523655 were characterized by inhibition of the expression of RTP801 at the molecular level and reduction of CNV lesions at the pathobiological level. The relationship between the pharmacodynamics and pharmacokinetics of PF-04523655 was profiled in rodent models of STZ-induced diabetes. The nonclinical information presented in this article may prove useful to guide interpretation of efficacy data from on-going clinical studies with PF-04523655 and inform dose and regimen selection in future clinical studies.

Acknowledgments

First presented in poster form at the annual meeting of the Association for Research in Vision and Ophthalmology, Fort Lauderdale, Florida, May 2010 (Johnson TR. *IOVS* 2010;51:ARVO E-Abstract 2442 and Rittenhouse KD, et al. *IOVS* 2010;51:ARVO E-Abstract 6447) and May 2011 (Rittenhouse KD, et al. *IOVS* 2011;52:ARVO E-Abstract 5641). PV receives royalties from the University of Washington Center for Commercialization, the licensor of the SAAM II software.

Disclosure: **K.D. Rittenhouse**, Pfizer, Inc. (E); **T.R. Johnson**, Pfizer, Inc. (E); **P. Vicini**, Pfizer, Inc. (E), P; **B. Hirakawa**, Pfizer, Inc. (E); **D. Kalabat**, Pfizer, Inc. (E); **A.H. Yang**, Pfizer, Inc. (E); **W. Huang**, Pfizer, Inc. (E); **A.S. Basile**, Pfizer, Inc. (E)

References

1. Tolentino MJ, Brucker AJ, Fosnot J, et al. Intravitreal injection of vascular endothelial growth factor small interfering RNA inhibits growth and leakage in a nonhuman primate, laser-induced model of choroidal neovascularization. *Retina*. 2004; 24:132–138.
2. Nguyen QD, Schachar RA, Nduaka CI, et al. MONET Clinical Study Group. Evaluation of the siRNA PF-04523655 versus ranibizumab for the treatment of neovascular age-related macular degeneration (MONET Study). *Ophthalmol*. 2012; 119:1867–1873.
3. Nguyen QD, Schachar RA, Nduaka CI, et al. Dose-ranging evaluation of intravitreal siRNA PF-04523655 for diabetic macular edema (the DEGAS Study). *Invest Ophthalmol Vis Sci*. 2012;53:7666–7674.
4. Kaiser PK, Symons RC, Shah SM, et al. RNAi-based treatment for neovascular age-related macular degeneration by Sirna-027. *Am J Ophthalmol*. 2010;150:33–39.
5. Corradetti MN, Inoki K, Guan KL. The stress-induced proteins RTP801 and RTP801L are negative regulators of the mammalian target of rapamycin pathway. *J Biol Chem*. 2005;280: 9769–9772.

6. Brugarolas J, Lei K, Hurley RL, et al. Regulation of mTOR function in response to hypoxia by REDD1 and the TSC1/TSC2 tumor suppressor complex. *Genes Dev.* 2004;18:2893–2904.
7. Ellisen LW. Smoking and emphysema: the stress connection. *Nat Medicine*. 2010;16:754–755.
8. Shoshani T, Faerman A, Mett I, et al. Identification of a novel HIF 1-responsive gene, RTP801, involved in apoptosis. *Mol Cell Biol*. 2002;22:2283–2293.
9. Ellisen LW, Ramsayer KD, Johannessen CM, et al. REDD1, a developmentally regulated transcriptional target of p63 and p53, links p63 to regulation of reactive oxygen species. *Mol Cell*. 2002;10:995–1005.
10. Lee DU, Huang W, Rittenhouse KD, Jessen B. Retina expression and cross-species validation of gene silencing by PF-655, a small interfering RNA against RTP801 for the treatment of ocular disease. *J Ocul Pharmacol Ther.* 2012; 28:222–230.
11. Malagelada C, Zong HJ, Lloyd AG. RTP801 is induced in Parkinson's disease and mediates neuron death by inhibiting Akt phosphorylation/activation. *J Neurosci*. 2008;28:14363–14371.
12. Malagelada C, Elizabeth JR, Biswas SC, et al. RTP801 is elevated in Parkinson brain substantia nigral neurons and mediates death in cellular modes of Parkinson's diseases by a mechanism involving mTOR inactivation. *J Neurosci*. 2006; 26:9996–10005.
13. Yoshida T, Mett I, Bhunia AK, et al. RTP801, a suppressor of mTOR signaling, is an essential mediator of cigarette smoke–induced pulmonary injury and emphysema. *Nat Med*. 2010; 16:767–773.
14. Lang CH, Frost RA, Vary TC. Acute alcohol intoxication increases REDD1 in skeletal muscle. *Alcohol Clin Exp Res*. 2008;32:796–805.
15. Sim DA, Keane PA, Zarranz-Ventura J, et al. The effects of macular ischemia on visual acuity in diabetic retinopathy. *Invest Ophthalmol Vis Sci*. 2013;54:2353–2360.
16. Xu H, Chen M, Forrester JV. Para-inflammation in the aging retina. *Prog Retin Eye Res*. 2009;28:348–368.
17. Klein R, Klein BE, Knudtson MD, Wong TY, Shankar A, Tsai MY. Systemic markers of inflammation, endothelial dysfunction, and age-related maculopathy. *Am J Ophthalmol*. 2005; 140:35–44.
18. Brafman A, Mett I, Shafir M, et al. Inhibition of oxygen-induced retinopathy in RTP801 deficient mice. *Invest Ophthalmol Vis Sci*. 2004;15:3796–3805.
19. Phase II Open Label Multicenter Study For Age Related Macular Degeneration Comparing PF-04523655 Versus Lucentis In The Treatment Of Subjects With CNV (MONET Study). Available at: ClinicalTrials.gov. Identifier: NCT00713518.
20. Gabrielsson J, Weiner D. *Effect-Compartment Model in Pharmacokinetic and Pharmacodynamic Data Analysis: Concepts and Applications*. 2nd ed. Stockholm, Sweden: Swedish Pharmaceutical Press; 1997:210–222.
21. Turabelidze A, Guo S, DiPietro LA. Importance of Housekeeping gene selection for accurate RT-qPCR in a wound healing model. *Wound Repair Regen*. 2010;18:460–466.
22. Van den Berg A, Mols J, Han J. RISC-target interaction: cleavage and translational suppression. *Biochimt Biophys Acta*. 2008; 1779:668–677.
23. Bartlett DW, Davis ME. Insights into the kinetics of siRNA-mediated gene silencing from live-cell and live-animal bioluminescent imaging. *Nucleic Acids Res*. 2006;34:322–333.
24. Léveillard T, Mohand-Saïd S, Lorentz O, et al. Identification and characterization of rod-derived cone viability factor. *Nat Genet*. 2004;36:755–759.

Investigative Ophthalmology & Visual Science